

D2.3 Database of descriptors of theoretically developed molecular models and final list of the most promising SOEC components

Report name: D2.3 Database of descriptors of theoretically developed molecular models and final list of the most promising SOEC components

Version number: 1.2

Due date for deliverable: 30-04-2024

Actual submission date: 30-04-2024

Lead beneficiary: QSAR Lab

Classification: PU



This project has received funding from the European Union's Horizon Europe research and innovation programme under grant agreement N°101058784

The present publication reflects only the author's views and the European Union is not liable for any use that may be made of the information contained therein

DOCUMENT CONTROL PAGE

Author: Alicja Mikołajczyk
Version number: 1.2
Date: 24-04-2024
Modified by: Marijke Jacobs

REVISION HISTORY

Version	Date	Author/Reviewer	Notes
1.0	24-04-2024	Alicja Mikołajczyk / QSAR Lab	First draft
1.1	26-04-2024	Marijke Jacobs / VITO	Revised
1.2	30-04-2024	Marijke Jacobs / VITO	Approved by all partners

EXECUTIVE SUMMARY

The purpose of this deliverable D2.3 is to obtain database of descriptors of theoretically developed molecular models and final list of the most promising SOEC components. The D2.3 is summary of the results derived from quantum mechanical calculations of possible SOEC structures, obtained within Task 2.2. The calculations of 165 potential SOEC structures was prepared by using Gaussian16 computational chemistry software package using density functional theory (DFT) obtained at the MN15/LANL2DZ/6-31G level. As a result of a task, a 3 sets of quantum mechanical descriptors were obtained. First set of descriptors is associated with the distribution of electron density and the electronic stability of the system, second set with physicochemical properties of the system and the last with spatial attributes of molecules. Numerical values of descriptors are included in appendix. The obtained datasets were then used for virtual screening of the most promising SOEC components. The most optimal structures of SOEC (anode part) were selected based on virtual screening approach from designed virtual library that contain theoretically developed 165 potential SOEC structures.

TABLE OF CONTENTS

List of Abbreviations	5
1 INTRODUCTION	6
1.1 Objectives of WP2 work package	7
1.2 Description of Task 2.2 Materials modeling and physic-based models development	7
2 METHODOLOGY OF QUANTUM MECHANICAL CALCULATIONS	8
2.1 Determining the multiplicity of the ground electronic state (QSAR Lab)	8
2.2 Quantum mechanical descriptions calculations (QSAR Lab)	13
3 SELECTION OF THE MOST PROMISING SOEC (ANODE) STRUCTURES	17
4 CONCLUSIONS & NEXT STEPS	21
5 INDEX OF ALL FIGURES	22
6 REFERENCES	23

List of Abbreviations

Abbreviation	Definition
AI	Artificial Intelligence
ASE	Atomic Simulation Environment
CWA	CEN Workshop Agreement
DFT	density functional theory
EMMC	European Materials Modelling Council
M3GNet	Materials Graph Network
MD	molecular dynamics
ML	Machine Learning
MM	molecular models
MODA	MOdelling DATA
MSD	Mean Square Displacement
PGM	Platinum Group Metals
REE	Rare Earth Elements
SOEC	Solid Oxide Electrolyser Cell
SOEC	Solid oxide electrolyzer cell
SOFC	Solid oxide fuel cell
SPF	structure-property-function
SPH	structure-property-hazard
SSbD	Safe And Sustainable by Design
YSZ	Yttria-stabilized zirconia

1 INTRODUCTION

The NOUVEAU project is aimed at the development of solid oxide cells with novel electrode materials and interconnects with a reduced amount of REE, PGM, and Cr by employing innovative coating methodologies and modelling combined with sustainable-by-design aspects and recycling options.

The main challenge in the design process of efficient SOEC is that there are thousands of possible combinations of structural features. Thus, it is irrational to experimentally synthesize and test all of them to find the most effective materials and interconnects. The development of SOEC so far was based on subjective experts' expectations and very narrow investigations rather than systematic studies of a wide space of possible solutions. We hypothesize that this challenge can be faced by the application of appropriate computational methods based on materials modeling (physic-based models) and virtual design (data-based models). The virtual design of new potential materials for sustainable development requires the appropriate determination of different components assembled in the final device. These phenomena are governed by the physicochemical properties of the materials, mainly related to the optoelectronic and redox characteristics that directly affect the materials' performance.

To design and predict new SOEC materials for sustainable development applications, density functional theory (DFT) is considered nowadays as a precious and reliable computational tool. It can significantly help experimentalists develop a rational design of new suitable materials for this purpose by computing the challenging fundamental physicochemical parameters, since some of them are difficult to be obtained by experiments. Although several theoretical studies appeared on the bulk features of materials, there has been no systematic work on the characteristics of their surfaces. A deep investigation of the various possible surfaces and the relevant properties of each surface to redox reactions is highly required to identify the discrepancy and the main factors limiting the performance and propose the most appropriate way to overcome such limitation. Thus, in this Deliverable we present a list of descriptors of possible SOEC structures, obtained with quantum mechanical calculations, using density functional theory (DFT) obtained at the MN15/LANL2DZ/6-31G level. Further to

study the electrochemical properties such as diffusion coefficient and ionic conductivity of the electrode materials, Molecular dynamic simulations were performed using AI trained models. The most optimal structures of SOEC (anode part) were selected based on virtual screening approach from designed virtual library that contain theoretically developed 165 potential SOEC structures.

1.1 Objectives of WP2 work package

The main objectives of WP2 are:

- Identification of structural data gaps (based on previous and ongoing EU projects) as well as data needs for molecular models' development (MM) and for predictive structure-property-function (SPF) and structure-property-hazard (SPH) relationship models development (ML and AI).
- Collection and management of the in silico methodologies and data from public sources and existing EU-completed and ongoing projects reliable for developing SSbD tools and novel materials.

1.2 Description of Task 2.2 Materials modeling and physic-based models development

- Development of virtual library that contains combinatorically generated virtual compounds (derivatives of solid oxide cells with variety of doping and structures, e.g., defects).
- Development and integration of a multi-scale material modelling (MM) framework for assessing physicochemical properties of investigated systems (all models and model interconnections will be documented according to the MOdelling DAta (MODA) approach, as documented in the CEN Workshop Agreement (CWA) about "Materials modelling - terminology, classification and metadata" (<https://www.cen.eu/News/Workshops/Pages/WS-2017-012.aspx>), which has been proposed by the European Materials Modelling Council (EMMC, <https://emmc.info/>).
- Development of physics-based models and modeling (conducted at one or more of the four levels: electronic, atomistic, mesoscopic, and continuum level)

for accurate for predicting, assessing, and characterizing specific properties and descriptors of selected individual components and interconnects layers at the early stage of materials design (before synthesis).

- Embedding of physics-base models in phenomenological model for large scale design and techno economic assessment of the process.

2 METHODOLOGY OF QUANTUM MECHANICAL CALCULATIONS

2.1 Determining the multiplicity of the ground electronic state (QSAR Lab)

Based on developed molecular modelling methodology, 165 molecular models of possible SOEC parts (anode) were virtually designed and developed. The preliminary molecular models were built based on the doped and pristine form of Brownmillerite crystal structure, Figure 1.

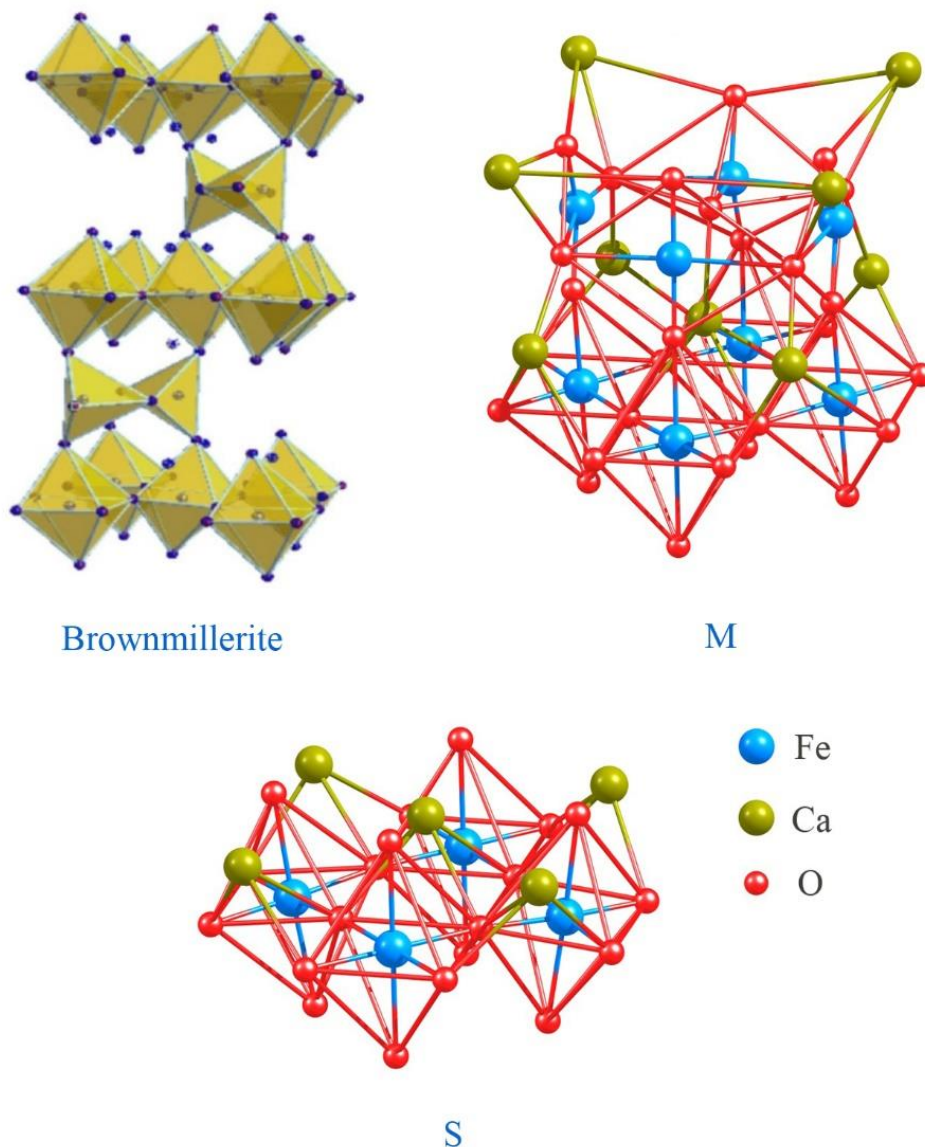


Figure 1. Schematic Brownmillerite crystal structure and two fragments (M and S) selected for calculations.

Modifications were selected according to the available literature data and knowledge obtained within other NOUVEAU Project work packages. Designed structures were developed based on Brownmillerite crystal structure, with Fe atoms substituted with Co and/or Mn atoms, as well as replacing Ca atoms with La or Bi atoms (Figure 2).

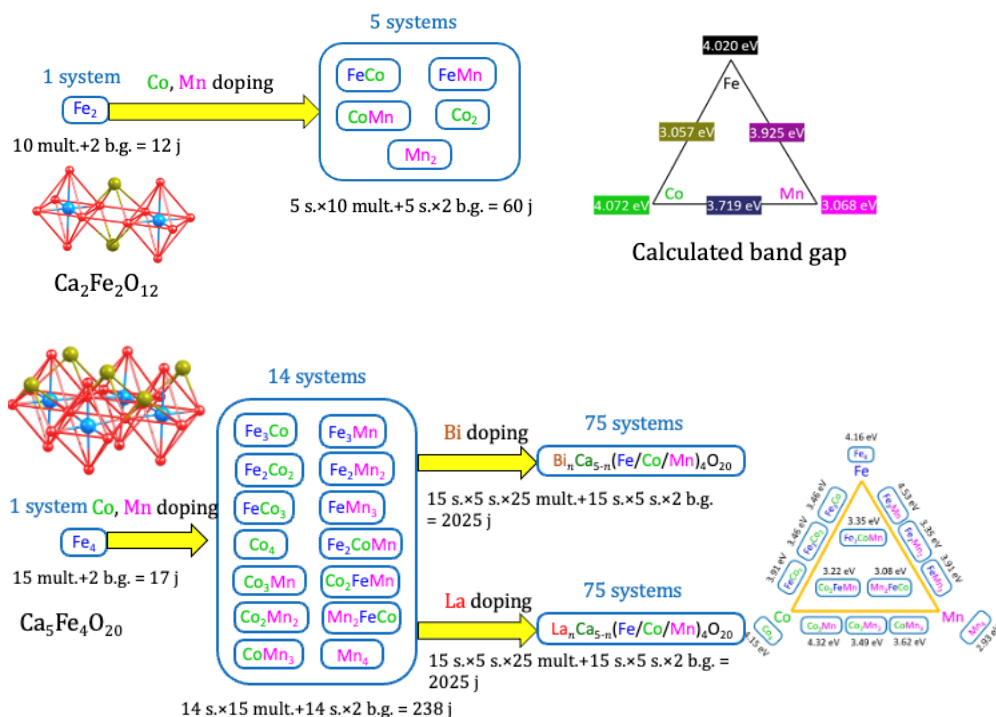


Figure 2. Schematic methodology for molecular modeling of brownmillerite crystal structure and two fragments (M and S) selected for calculations.

Because performing quantum chemical electronic structure calculations for such extensive systems is unfeasible, we needed to downsize the Brownmillerite structure. Nonetheless, we ensured that the fragments utilized in the computations remained indicative and preserved the essential structural characteristics of the examined crystals. Based on assumption of downsize the brownmillerite structure, we built two systems, distinguished with different sizes. Larger M structure contained 46 atoms (29 oxygen atoms, 9 Ca-positions and 8 Fe-positions). Smaller S structure was built of 29 atoms (20 oxygen atoms, 5 Ca-positions and 4 Fe-positions). Reference Brownmillerite structure, as well M and S structures are shown on Figure 1. To evaluate how substituting Fe atoms with Co and/or Mn atoms, and replacing Ca atoms with La or Bi atoms, affects the properties of the system, we chose a specific segment of the Brownmillerite structure, denoted as S. This choice allows us to consider all possible combinations of dopants (Table 1, Figure 2).

Table 1. Summary of molecular modeling of brownmillerite crystal structure and two fragments (M and S) selected for calculations.

System	Ground state multiplicity $2S+1$	Band gap	Comment (code)
$\text{Ca}_5\text{Fe}_4\text{O}_{20}$	23	4.16 eV	No doping (FeFeFeFe, XS_0)
$\text{Ca}_5\text{Fe}_3\text{CoO}_{20}$	30	3.46 eV	(FeFeFeCo, XS_1)
$\text{Ca}_5\text{Fe}_2\text{Co}_2\text{O}_{20}$	27	3.46 eV	(FeFeCoCo, XS_2)
$\text{Ca}_5\text{FeCo}_3\text{O}_{20}$	18	3.91 eV	(FeCoCoCo, XS_3)
$\text{Ca}_5\text{Co}_4\text{O}_{20}$	27	4.15 eV	(CoCoCoCo, XS_4)
$\text{Ca}_5\text{Fe}_3\text{MnO}_{20}$	22	4.53 eV	(FeFeFeMn, XS_5)
$\text{Ca}_5\text{Fe}_2\text{Mn}_2\text{O}_{20}$	11	3.35 eV	(FeFeMnMn, XS_6)
$\text{Ca}_5\text{FeMn}_3\text{O}_{20}$	8	3.91 eV	(FeMnMnMn, XS_7)
$\text{Ca}_5\text{Mn}_4\text{O}_{20}$	11	2.93 eV	(MnMnMnMn, XS_8)
$\text{Ca}_5\text{Fe}_2\text{CoMnO}_{20}$	9	3.35 eV	(FeFeCoMn, XS_9)
$\text{Ca}_5\text{FeCo}_2\text{MnO}_{20}$	22	3.22 eV	(FeCoCoMn, XS_10)
$\text{Ca}_5\text{FeCoMn}_2\text{O}_{20}$	8	3.08 eV	(FeCoMnMn, XS_11)
$\text{Ca}_5\text{Co}_2\text{Mn}_2\text{O}_{20}$	19	3.49 eV	(CoCoMnMn, XS_12)
$\text{Ca}_5\text{CoMn}_3\text{O}_{20}$	11	3.62 eV	(CoMnMnMn, XS_13)
$\text{Ca}_5\text{Co}_3\text{MnO}_{20}$	9	4.32 eV	(CoCoCoMn, XS_14)

All structures were investigated with GAUSSIAN 16 computational chemistry software package and MultiWFN multifunctional wavefunction analyzer, for establish multiplicity of all the systems and further calculations of quantum mechanical descriptors. For each of the 165 compounds under consideration, characterized as open-shell systems, their electronic states exhibit different multiplicities ($2S+1$). As it is not feasible to determine the most optimal multiplicity a priori, particularly for minimizing the system's total energy, we conducted calculations for a range of $2S+1$ values, spanning from 1 to 40.

As an example, (this type of calculations was performed for each 165 systems), we present exemplary dependence of electronic energy on multiplicity for $\text{La}_4\text{Ca}_1\text{Fe}_3\text{Mn}_1\text{O}_{20}$ system.

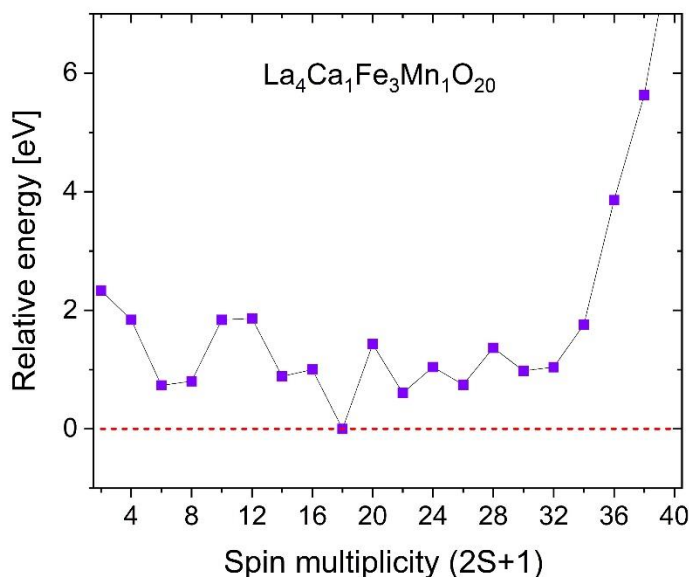


Figure 2. Relative electronic energies of the representative La₄Ca₁Fe₃Mn₁O₂₀ system corresponding to various multiplicities (in this case, 2S+1=17 multiplicity corresponds to the ground electronic state).

This comprehensive approach enabled us to identify the preferred multiplicity for each specific case. Implementing this method for every system entailed calculating the electronic energy across a total of 3300 electronic states. Through this exhaustive process, we determined the multiplicity of the ground electronic state for each of the 165 compounds. Calculations of the descriptors were conducted, only for ground state for each of system. Additionally, we noted that lowest energy multiplicity of investigated systems was around 26-28. Distribution of multiplicities of investigated structures is shown on Figure 3.

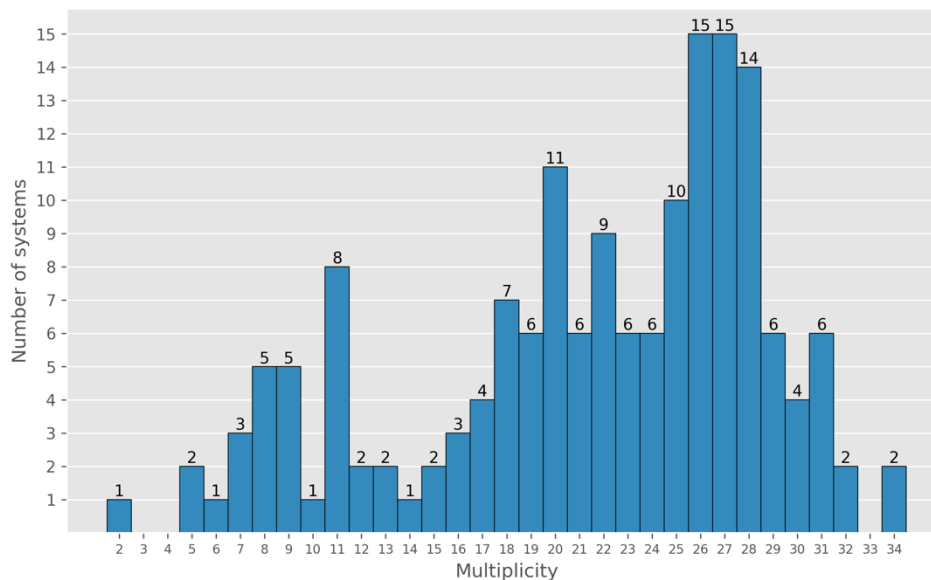


Figure 3. Histogram representing distribution of the multiplicities of the ground electronic states of investigated systems.

2.2 Quantum mechanical descriptions calculations (QSAR Lab)

Next step for obtaining quantum mechanical descriptions was to prepare calculations for systems with lowest energy state multiplicities. Based on knowledge obtained in previous step, we characterized the systems, based on the electron density obtained at the MN15/LANL2DZ/6-31G level [1-8]. The calculations were performed using Gaussian16 computational chemistry software package [8] and MultiWFN multifunctional wavefunction analyzer [9]. Based on the calculation results, we obtained descriptors, listed in the table below.

Table 2. List of descriptors with its abbreviations and units, used in sheet in Appendix 1.

Descriptor	Descriptor abbreviation
eigenvalue of the highest singly occupied molecular orbital	SOMO [eV]
fundamental band gap	Band gap [eV]
dipole moment	Dipole moment [D]
quadrupole moment	Quadrupole moment [D*Å]
ionization potential	IP [eV]
electron affinity	VAE [eV]

Descriptor	Descriptor abbreviation
electronic spatial extent	Electronic spatial extent [a.u.]
Mulliken absolute electronegativity	Electronegativity [eV]
Pearson's absolute chemical hardness	Hardness [eV]
Pearson's absolute chemical softness	Softness [1/eV]
Parr's electrophilicity index	Electrophilicity [eV]
molecular volume	Volume [Angstrom^3]
polar surface area	Nonpolar surface area ($ ESP \leq 10$ kcal/mol) [%]
non-polar surface area	Polar surface area ($ ESP > 10$ kcal/mol) [%]
molecular polarity index	Molecular polarity index (MPI) [kcal/mol]
magnetic moment	Magnetic moment $\times 10^{-24}$ [J/T]
Position Ca charges [a.u.]	Mean of partial charges for atoms in Ca position in neutral
Position Fe charges [a.u.]	Mean of partial charges for atoms in Fe position in neutral
Position O charges [a.u.]	Mean of partial charges for atoms in O position in neutral
Position Ca charges [a.u.] (cation)	Mean of partial charges for atoms in Ca position in cation
Position Fe charges [a.u.] (cation)	Mean of partial charges for atoms in Fe position in cation
Position O charges [a.u.] (cation)	Mean of partial charges for atoms in O position in cation
Position Ca charges [a.u.] (anion)	Mean of partial charges for atoms in Ca position in anion
Position Fe charges [a.u.] (anion)	Mean of partial charges for atoms in Fe position in anion
Position O charges [a.u.] (anion)	Mean of partial charges for atoms in O position in anion

Moreover, for each ground electronic state in the case of all 165 systems, we performed additional calculations in the presence of the external electric dipole field ($E_1=0.002$ au and $E_2=0.004$ au) applied independently in three directions (i.e., along the x, y, and z axis). Additionally, we calculated descriptors which are ratio external electric dipole to molecule volume. Introducing external electric field calculations enabled us to determine the induced changes in system polarity for each of the three directions. As the macroscopic polarization (P) of the molecular

system is defined as the ratio of the induced polarization change to the system's volume, we thereby reproduced a measurable quantity, which we also included in the group of molecular descriptors. Furthermore, performing similar calculations for various intensities of the external electric field E allowed us to expand the set of polarization descriptors. Additionally, we calculated numerical derivatives (P') of the polarization function $P=f(E)$ at an arbitrarily chosen point, $E=0.002$ au. This, in accordance with the interpretation of the derivative function, provided us with information about the rate of increase of the P function (the numerical derivative value was also included in the set of descriptors characterizing all 165 systems).

Calculated descriptors (collected in Tables 2 and 3) can be classified into several categories based on their significance and the properties they depict. One category encompasses descriptors associated with the distribution of electron density and the electronic stability of the system, including the system's capacity to bind an excess electron. This category includes eigenvalues of singly occupied molecular orbitals, ionization potential, electron affinity, electronic spatial extent (for neutral system as well cation and anion form), differences of electronic spatial extent between neutral and cation as well neutral and anion, and the fundamental band gap. We also calculated descriptors for all atoms in positions of calcium, iron, and oxygen, as a means of partial charges of individual atoms, present in particular position. These calculations were prepared for neutral, cation and anion form, as well as the differences between neutral and cation as well neutral and anion. The second category comprises descriptors linked to the physicochemical properties of the system under examination. This set encompasses the electric dipole moment, electric quadrupole moment, magnetic moment, Mulliken absolute electronegativity, Pearson's absolute chemical hardness and softness, Parr's electrophilicity index, and molecular polarity index. The third category consists of descriptors concerning the spatial attributes of molecules, such as their shape, volume, and surface area (including information about both polar and non-polar surface areas). Lastly, the fourth category comprises descriptors related to how the molecular system responds to external perturbations, such as an external electric field. This category encompasses the complete set of

descriptors that characterize macroscopic polarization in various directions and its derivative functions.

Table 3. List of polarity descriptors with its abbreviations and units, used in sheet in Appendix 1.

Descriptor	Descriptor abbreviation
Dipole moment of system under external electric dipole field ($E_1=0.002$ a.u.) along the x axis	μ_{px} [D]
Dipole moment of system under external electric dipole field ($E_1=0.002$ a.u.) along the y axis	μ_{py} [D]
Dipole moment of system under external electric dipole field ($E_1=0.002$ a.u.) along the z axis	μ_{pz} [D]
Dipole moment of system under external electric dipole field ($E_1=0.004$ a.u.) along the x axis	μ_{p2x} [D]
Dipole moment of system under external electric dipole field ($E_1=0.004$ a.u.) along the y axis	μ_{p2y} [D]
Dipole moment of system under external electric dipole field ($E_1=0.004$ a.u.) along the z axis	μ_{p2z} [D]
Dipole moment of system under external electric dipole field ($E_1=0.0021$ a.u.) along the z axis	μ_{oz} [D]
Dipole moment of system under external electric dipole field ($E_1=0.0019$ a.u.) along the z axis	μ_{qz} [D]
Dipole moment of system under external electric dipole field ($E_1=0.002$ a.u.) along the x axis divided by molecule volume	$P_x(1)$ [D/Å ³]
Dipole moment of system under external electric dipole field ($E_1=0.002$ a.u.) along the y axis divided by molecule volume	$P_y(1)$ [D/Å ³]
Dipole moment of system under external electric dipole field ($E_1=0.002$ a.u.) along the z axis divided by molecule volume	$P_z(1)$ [D/Å ³]

Descriptor	Descriptor abbreviation
Dipole moment of system under external electric dipole field ($E_1=0.004$ a.u.) along the x axis divided by molecule volume	$P_x(2)$ [$D/\text{\AA}^3$]
Dipole moment of system under external electric dipole field ($E_1=0.004$ a.u.) along the y axis divided by molecule volume	$P_y(2)$ [$D/\text{\AA}^3$]
Dipole moment of system under external electric dipole field ($E_1=0.004$ a.u.) along the z axis divided by molecule volume	$P_z(2)$ [$D/\text{\AA}^3$]
Numerical derivative for x axis external electric dipole field	$\Delta P_x/\Delta E$
Numerical derivative for y axis external electric dipole field	$\Delta P_y/\Delta E$
Numerical derivative for z axis external electric dipole field	$\Delta P_z/\Delta E$

3 SELECTION OF THE MOST PROMISING SOEC (ANODE) STRUCTURES

The chemoinformatic analysis combined with developed database of theoretically calculated descriptors were performed for virtual screening and the design process of the SOEC (anode) part. The results presented here are the first part of developed theoretical methodology that will support design of the efficient SOEC at the early stage (before synthesis).

The virtual design process is based on several steps. At first, a database of possible anode structures was generated. As described in section 1-2, the structures were based on Brownmillerite crystal structure (Figure 1) in which Fe atoms were substituted with Co and/or Mn atoms, whereas Ca atoms were replaced with La or Bi atoms. The properties of such modified systems were investigated.

Thus, for the substitution of four iron atoms with Co and Mn dopants, 15 possible combinations were virtually designed and theoretically characterized. Similarly, in the case of replacing five Ca atoms in the S structure with dopants of the same type (La or Bi), there 75 possible combinations in both scenarios were designed

and theoretically characterized. In total, this results in 165 S-type virtually generated systems, differing in the content of the mentioned metals. Consequently, it enables the determination of selected physicochemical properties based on the stoichiometry (molar fractions) indicating the percentage content of individual components. Since the selection of specific Fe or Ca atoms to be replaced by Mn and Co dopants or La and Bi dopants, respectively, was arbitrary, our strategy involved choosing atom locations where substitution with a dopant would result in the highest possible symmetry point group.

At the second stage, dataset of 51 descriptor (61 descriptors together with its numerical derivatives) were obtained. Then, the final matrix with 165 theoretically designed structures and 61 descriptors (together 1065 datapoints, Appendix A) was obtained for virtual screening and optimal SOEC structure (anode part) selection.

In the final stage, the Principal Component Analysis (PCA) with distinction for modified and non-modified structures was employed to visualize the studied dataset and investigate possible patterns and similarities of the SOEC structure (anode part), Figure 4.

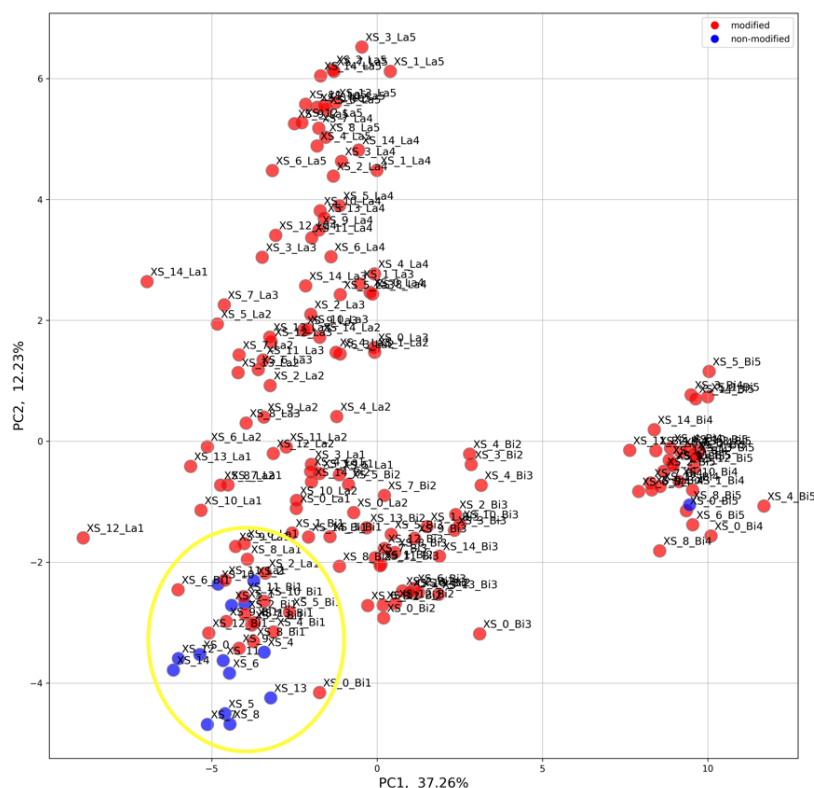


Figure 4. Principal Component Analysis score plot.

Interestingly, results provided by experimental group (WP3) indicate that the structure $\text{Ca}_2\text{Fe}_{0.5}\text{Mn}_{1.5}\text{O}_{6-\delta}$ showed good mixed ionic-electronic conductivity, promising oxygen permeability, thermal expansion coefficients (TECs) compatible with typical solid electrolytes and low area specific resistance (ASR) values. This structure is similar to theoretically designed XS_7 structure ($\text{Ca}_5\text{FeMn}_3\text{O}_6$), which contain the same molar ration of Fe to Mn atoms (1:3). The experimental results indicate also that the electronic conductivity was improved by doping with Bi, Y or La on the Ca site. This led to an ASR of only $0.74 \text{ } \Omega \cdot \text{cm}^2$ at $800 \text{ } ^\circ\text{C}$ or the pure $\text{Ca}_{1.9}\text{Bi}_{0.1}\text{Fe}_{0.5}\text{Mn}_{1.5}\text{O}_{6-\delta}$. This structure is similar to theoretically designed system XS_7_Bi1, which contain the same molar ration of Fe to Mn atoms (equal to 1:3), at the same time, the system has same molar ratio of Bi:Ca (equal to 1:4). As a conclusion, the compounds in yellow-marked group should be specifically investigated in further steps. All these compounds are listed in Table 4.

Table 4. List of structures designated to further investigations

Structure abbreviation	Total formula
XS_0	$\text{Ca}_5\text{Fe}_4\text{O}_{20}$
XS_0_Bi1	$\text{Ca}_4\text{BiFe}_4\text{O}_{20}$
XS_2_La1	$\text{Ca}_4\text{LaFe}_2\text{Co}_2\text{O}_{20}$
XS_2_La2	$\text{Ca}_3\text{La}_2\text{Fe}_2\text{Co}_2\text{O}_{20}$
XS_2_Bi1	$\text{Ca}_4\text{BiFe}_2\text{Co}_2\text{O}_{20}$
XS_4	$\text{Ca}_5\text{Co}_4\text{O}_{20}$
XS_4_Bi1	$\text{Ca}_4\text{BiCo}_4\text{O}_{20}$
XS_5	$\text{Ca}_5\text{Fe}_3\text{MnO}_{20}$
XS_5_Bi1	$\text{Ca}_4\text{BiFe}_3\text{MnO}_{20}$
XS_6	$\text{Ca}_5\text{Fe}_2\text{Mn}_2\text{O}_{20}$
XS_6_La1	$\text{Ca}_4\text{LaFe}_2\text{Mn}_2\text{O}_{20}$
XS_6_Bi1	$\text{Ca}_4\text{BiFe}_2\text{Mn}_2\text{O}_{20}$
XS_7	$\text{Ca}_5\text{FeMn}_3\text{O}_{20}$
XS_7_Bi1	$\text{Ca}_4\text{BiFeMn}_3\text{O}_{20}$
XS_8	$\text{Ca}_5\text{Mn}_4\text{O}_{20}$
XS_8_La1	$\text{Ca}_4\text{LaMn}_4\text{O}_{20}$
XS_8_Bi1	$\text{Ca}_4\text{BiMn}_4\text{O}_{20}$
XS_9_La1	$\text{Ca}_4\text{LaFe}_2\text{MnCoO}_{20}$
XS_9_Bi1	$\text{Ca}_4\text{BiFe}_2\text{MnCoO}_{20}$
XS_10	$\text{Ca}_5\text{FeMnCo}_2\text{O}_{20}$
XS_10_Bi1	$\text{Ca}_4\text{BiFeMnCo}_2\text{O}_{20}$
XS_11	$\text{Ca}_5\text{FeMn}_2\text{CoO}_{20}$
XS_12	$\text{Ca}_5\text{Mn}_2\text{Co}_2\text{O}_{20}$
XS_12_Bi1	$\text{Ca}_4\text{BiMn}_2\text{Co}_2\text{O}_{20}$
XS_13	$\text{Ca}_5\text{Mn}_3\text{CoO}_{20}$
XS_13_Bi1	$\text{Ca}_4\text{BiMn}_3\text{CoO}_{20}$
XS_14	$\text{Ca}_5\text{MnCo}_3\text{O}_{20}$

4 CONCLUSIONS & NEXT STEPS

MD simulations for NOUVEAU based materials are underway which is based on Ca, Fe, La, Mn based oxides. Phenomena based modelling for the cell level efficiency based on the novel materials with enhanced electrochemical properties predicted in first part.

In parallel, the multiscale modelling will be performed using phenomena based equations and applying the physical properties calculated in the first part to calculate the single cell efficiency for the ion conductivity. This approach will include mainly the CFD modelling and simulation and optimization of cell level parameters. Finally, stack level modelling, process and energy optimization of large scale implementations of the SOEC technology based on novel materials.

Thus to summarize, within deliverable 2.3 the matrix of virtually generated SOEC models and the theoretically characterized structures were obtained. The matrix of 10 065 datapoints were created and will be used in the next step for Deliverable 2.5: Final list of the most promising compounds (i.e., those which present an optimal combination of specific features, efficiency, and functionality) that will finally synthesized, experimentally tested and validated (WP3/WP4).

In the next step developed virtual screening methodology integrated with Molecular Models (MM), Machine Learning (ML) and Artificial intelligence (AI) will be applied for mapping, analyzing, and selecting final SOEC components for future validation in line with the SSbD approach. The ML-based methods will be applied to develop Quantitative Structure - Activity/Properties Relationship models (so-called Structure-Property Function and Structure-Hazard-Function models), to be applied to predict desired properties/safety of newly designed SOEC components. The predictive model will be used to answer how the structure modification influences their behavior and how to manipulate the structure to obtained SOEC with desire properties.

5 INDEX OF ALL FIGURES

NUMBER	DESCRIPTION
1	Schematic Brownmillerite crystal structure and two fragments (M and S) selected for calculations
2	Relative electronic energies of the representative $\text{La}_4\text{Ca}_1\text{Fe}_3\text{Mn}_1\text{O}_{20}$ system corresponding to various multiplicities (in this case, $2S+1=17$ multiplicity corresponds to the ground electronic state)
3	Histogram representing distribution of the multiplicities of the ground electronic states of investigated systems
4	Mean square displacement value for the supercell of YSZ structure vs time

6 REFERENCES

- [1] H. S. Yu, X. He, S. L. Li and D. G. Truhlar, MN15: A Kohn-Sham Global-Hybrid Exchange-Correlation Density Functional with Broad Accuracy for Multi-Reference and Single-Reference Systems and Noncovalent Interactions, *Chemical Science* 2016, **7**, 5032-5051.
- [2] Hay, P. J.; Wadt, W. R. Ab Initio Effective Core Potentials for Molecular Calculations. Potentials for the Transition Metal Atoms Sc to Hg. *J. Chem. Phys.*, **1985**, *82*, 270-283.
- [2] Wadt, W. R.; Hay, P. J. Ab Initio Effective Core Potentials for Molecular Calculations. Potentials for Main Group Elements Na to Bi. *J. Chem. Phys.*, **1985**, *82*, 284-298.
- [3] Hay, P. J.; Wadt, W. R. Ab Initio Effective Core Potentials for Molecular Calculations. Potentials for K to Au Including the Outermost Core Orbitals. *J. Chem. Phys.*, **1985**, *82*, 299-310.
- [4] R. Ditchfield, W. J. Hehre, and J. A. Pople, "Self-Consistent Molecular Orbital Methods. 9. Extended Gaussian-type basis for molecular-orbital studies of organic molecules," *J. Chem. Phys.*, **54** (1971) 724.
- [5] M. M. Francl, W. J. Pietro, W. J. Hehre, J. S. Binkley, D. J. DeFrees, J. A. Pople, and M. S. Gordon, "Self-Consistent Molecular Orbital Methods. 23. A polarization-type basis set for 2nd-row elements," *J. Chem. Phys.*, **77** (1982) 3654-3665.
- [6] R. C. Binning Jr. and L. A. Curtiss, "Compact contracted basis-sets for 3rd-row atoms – GA-KR," *J. Comp. Chem.*, **11** (1990) 1206-1216.
- [7] V. A. Rassolov, J. A. Pople, M. A. Ratner, and T. L. Windus, "6-31G* basis set for atoms K through Zn," *J. Chem. Phys.*, **109** (1998) 1223-1229.
- [8] Gaussian 16, Revision C.01, Frisch, M. J. et al. Gaussian, Inc., Wallingford CT, **2016**.
- [9] Lu, T.; Chen, F. Multiwfn: A multifunctional wavefunction analyzer. *J. Comput. Chem.* **2012**, *33*, 580-592.
- [10] Butz, B.; Kruse, P.; Stoermer, H.; Gerthsen, D.; Mueller, A.; Weber, A.; Ivers-Tiffée, E. *Solid State Ionics* (2006), *177* (37-38), 3275-3284.
- [11] Kondoh, Junya; Kawashima, Tsuyoshi; Kikuchi, Shiomi; Tomii, Yoichi; Ito, Yasuhiko *Journal of the Electrochemical Society* (1998), *145* (5), 1527-1538.